Follow-up strategies for MEO observations

A. Hinze, T. Schildknecht, A. Vananti

1. Abstract

The Medium Earth Orbit (MEO) region becomes increasingly populated as new navigation satellite constellations are deployed or existing constellations are replenished with new satellites. As a consequence a growing number of space debris including small size objects must be expected. The Astronomical Institute of the University Bern (AIUB) performs survey campaigns to search for debris objects in MEO. The optical observations are performed with ESA's Zeiss 1-m telescope located at the Teide Observatory on Tenerife, Spain and with the 0.3-m ZimSMART telescope of the AIUB, located 10 km south of Bern, Switzerland.

To characterize debris objects their orbits must be determined and maintained over a sufficiently long time interval. For a successful recovery of detected objects in the subsequent night after the first detection, a preliminary orbit has to be determined and further follow-up observations within the same night have to be carefully scheduled.

In this paper we present the results of different observation strategies and discuss the quality of the orbits determined from initial observations and follow-up observations performed after different time intervals.

2. Introduction

Space debris has been recognized as a serious danger for operational satellites and manned space flight. The population of space debris in the Medium Earth Orbit (MEO) is increasing and, unlike the extensively studied Low Earth Orbit (LEO) region and the more recently examined Geostationary Earth Orbit (GEO) ring (Schildknecht et al., 2001, Schildknecht et al., 2004), the population in MEO is not so well investigated. Therefore, the Astronomical Institute of the University Bern (AIUB) started surveys in the MEO region with the ESA Space Debris Telescope (ESASDT) on Tenerife, Spain and with the Zimmerwald Small Aperture Robotic Telescope (ZimSMART) in Zimmerwald, Switzerland.

The main objective of these surveys, besides obtaining statistical information about the MEO population, is the determination of accurate orbits for a better characterization of the debris environment and for cataloguing. The latter task requires so-called "secured" orbits that guarantee a safe recovery of the objects after a few weeks. The objects could be inserted into a catalogue as soon as a "secured" orbit is available. To investigate the conditions for "secured" orbits in terms of follow-up observations, MEO orbits were simulated and the object recovery under various conditions was tested. The generated orbits were used to simulate observations and to illustrate the orbit improvement process from the object discovery up to the "secured" orbit. Ephemerides were computed to compare the simulated orbits with the ones determined from simulated observations. A similar procedure to investigate the different follow-up strategies for GEO and GTO objects is presented in Musci et al. (2004) and Musci et al. (2005), respectively. Additionally, in Musci et al. (2006) follow-ups strategies are discussed using multiple observation sites.

3. The process of orbit determination and improvement

An object is normally detected on two to four consecutive frames of a survey campaign of the ESASDT. From a single tracklet, only four of the six Keplerian

elements can be determined. A circular orbit is determined as a first approximation. As the length of the observation arc is usually very short (only a few minutes) a circular orbit often is of better quality than a general six-parameter orbit. The orbit parameters are determined with the method of least squares for three and more observations. If follow-up observations are available, after this circular orbit determination a general orbit improvement process is involved using all observations and all six orbital elements are determined. In the orbit determination process the perturbations due to the Earth's oblateness and the gravitational attraction of Sun and Moon are included if the observation arc is less than 24 hours. If observations arc is longer than 24 hours a more sophisticated model is used. This model additionally includes the Earth's potential coefficients up to terms of degree and order 12, the perturbations due to the Earth tides, the corrections due to general relativity, and a simple model for the direct radiation pressure (DRP). All methods for the orbit determination and propagation used for this work are described in Beutler (2004).

4. Simulations

In order to study the orbit improvement process, orbital elements for 100 different MEO objects were simulated (from now on called "true" orbits). The elements were varied randomly within the limits specified in Table 1.

Semimajor axis	20000 km < a < 30000 km
Eccentricity	0.00 < e < 0.05
Inclination	50° < i < 70°
R.A. of ascending node	25° < Ω < 35°
Argument of perigee	0° < ω < 360°

Table 1: Range of the orbital elements a, e, i, Ω, and ω used for the simulation of 100 MEO orbits.

The ranges are given by a hypothetical explosion population in a typical orbit of the existing navigation satellite constellation. These "true" orbits were then used to simulate observations. The object position for the simulated discovery observation was close to the meridian. An error of σ = 0.5" was assumed for the accuracy of the single observations. This value is a typical error for ESASDT observations. An observation tracklet consists always of four single observations with an arc length of one minute. The time interval between observations inside of one tracklet was set to 20 seconds for all tracklets. All simulated observation tracklets (discovery and follow-up tracklets) for a given object are based on same orbital elements. The simulated observations were used to determine circular and elliptical orbits. These orbits were propagated and compared with the "true" orbits to assess their quality.

Discovery observation

Four observations were simulated for the discovery tracklet. Circular orbits were determined using all four observations with an arc length of t = 1 min. The averages of the formal errors of the determined elements (from now on called "mean formal errors") are given in Table 2. The a posteriori rms m of the observations was determined for all simulations and its average is given in the last column of Table 2.

a	i	Ω	T_0	m
2490 m	$6.1° \times 10^{-3}$	$8.1° \times 10^{-3}$	2.25 s	0.29”

Table 2: Mean formal errors of the orbital elements and mean a posteriori rms m for the circular orbit determination representing the discovery observations to the perigee passing time.

In order to recover an object after a few hours it is necessary that the determined orbit represents the “true” orbit rather accurately during this time interval. Therefore ephemerides for each determined orbit were computed and the differences between the ephemerides of the determined orbit and the “true” orbit were calculated using

$$\Delta = \arccos\left(\sin\delta_t \sin\delta_d + \cos\delta_t \cos\delta_d \cos\Delta\alpha\right), \qquad (1)$$

where δ_t and δ_d are the declination values from the “true” and the determined orbit and $\Delta\alpha$ is the differences in right ascension α. The differences Δ as a function of time are shown in Figure 1. Each curve represents one of 100 simulated MEO objects. For all simulated orbits the differences are smaller than 0.5° within the first 30 minutes after the discovery. The differences have to be smaller than half of the Field Of View (FOV) of the instrument for a successful recovery. The results in Figure 1 show that most of the objects may be successfully recovered within 30 minutes with the ESASDT, which has a FOV of about 0.7°. With ZimSMART, which has a FOV of about 4.2°, a successful recovery after one hour is possible.

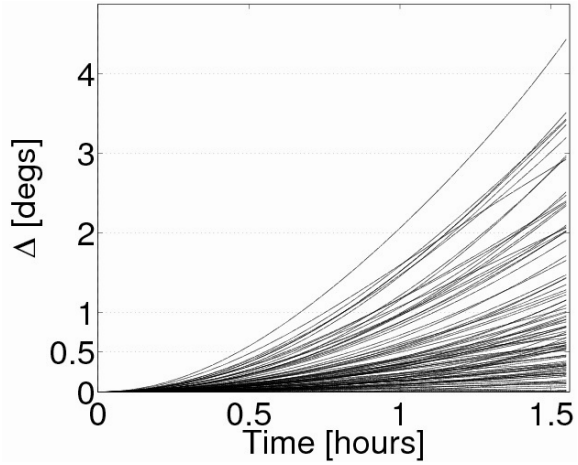

Figure 1: Difference Δ between “true” and circular orbit representing four discovery observations spanning one minute of time. Each curve represents the result for one of the 100 simulated MEO objects.

First and second follow-up observation sequences for ZimSMART

The next step consists of simulating follow-up observations. Based on the result from the previous section, observations after one hour were simulated and all the observations were used to determine new orbits. Observations arcs of one hour are long enough to determine elliptical orbits. The differences between orbits as a function of time are shown in Figure 2. Almost all differences are smaller than 0.3° within two hours and smaller than 2° within four hours.

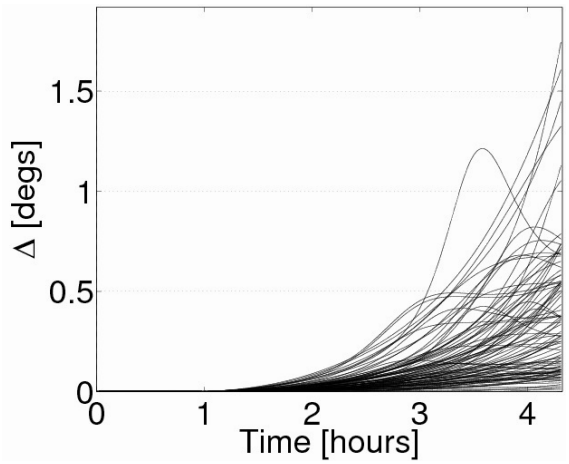

Figure 2: Difference Δ between "true" and elliptical orbit representing the discovery and the first follow-up observation spanning 1 hour of time. Each curve represents the result for one of the 100 simulated MEO objects.

A second follow-up observation during the same night is absolutely necessary for a successful recovery during the next nights. Therefore a second follow-up tracklet was simulated three hours after the discovery. The latter represents in general the latest possible follow-up because of the available observation time during the night. Figure 3 shows the differences between the "true" orbit and determined elliptical orbit. The mean formal errors and the mean a posteriori rms are given in Table 3 for the first follow-up (second row) and the second follow-up (third row). Note that the big error of T_0 is directly correlated with the error of the longitude of the perigee ω. This behaviour is a consequence of the small eccentricity.

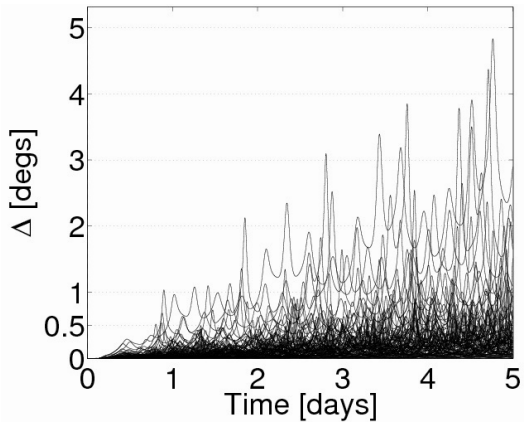

Figure 3: Difference Δ between "true" and elliptical orbit representing the discovery, first and second follow-up observations spanning 3 hours of time. Each curve represents the result for one of the 100 simulated MEO objects.

a	e	i	Ω	ω	T_0	m
6.3×10^4 m	1.1×10^{-3}	$4.2° \times 10^{-3}$	$7.2° \times 10^{-4}$	9.1°	972.5 s	0.3"
2.3×10^3 m	4.7×10^{-4}	$2.1° \times 10^{-4}$	$3.8° \times 10^{-5}$	0.7°	65.1 s	0.3"

Table 3: mean formal errors of the orbital elements and mean a posteriori rms for the elliptical orbit determination representing the first and the second follow-up observations.

First and second follow-up sequences for the ESASDT

For the ESASDT the time interval for follow-up observations has to be smaller because of a smaller FOV. Therefore a first follow-up tracklet was simulated 30 minutes after the discovery. All observations have been used again to determine elliptical orbits and the differences are shown in Fig. 4. Within two hours, all differences are smaller than 0.3°.

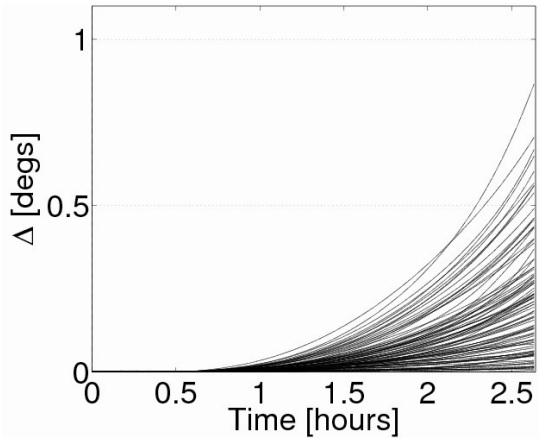

Figure 4: Difference Δ between "true" and elliptical orbit representing the discovery and the first follow-up observation spanning 30 minutes of time. Each curve represents the result for one of the 100 simulated MEO objetcs.

A second follow-up tracklet was assumed two hours after the discovery. All observations tracklets have been used to determine an elliptical orbit and the differences are shown in Fig. 5.

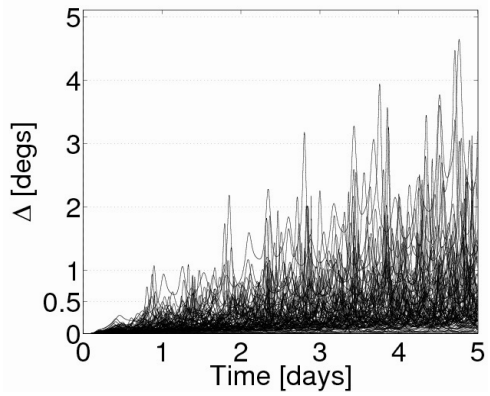

Figure 5: Difference Δ between "true" and elliptical orbit representing the discovery, first and second follow-up observations spanning 2 hours of time. Each curve represents the result for one of the 100 simulated MEO objects.

The mean formal errors and the mean a posteriori rms are given in Table 4 for the first follow-up (second row) and the second follow-up (third row).

a	e	i	Ω	ω	T_0	m
1.9×10^5 m	3.5×10^{-3}	$1.2° \times 10^{-2}$	$1.9° \times 10^{-3}$	20.0°	2071 s	0.3”
3.3×10^3 m	6.3×10^{-5}	$2.1° \times 10^{-4}$	$4.4° \times 10^{-5}$	0.37°	41.5 s	0.3”

Table 4: mean formal errors of the orbital elements and mean a posteriori rms *m* for the elliptical orbit determination representing the first and the second follow-up observations.

For both, ZimSMART and ESASDT, the differences after the second follow-up observations show significant peaks for some objects. To understand this behavior Monte Carlo simulation for a single object was performed with 50 different runs. The error of a single observation was again assumed to be $\sigma = 0.5$”. Figure 6 shows the results after the first and the second follow-up tracklet.

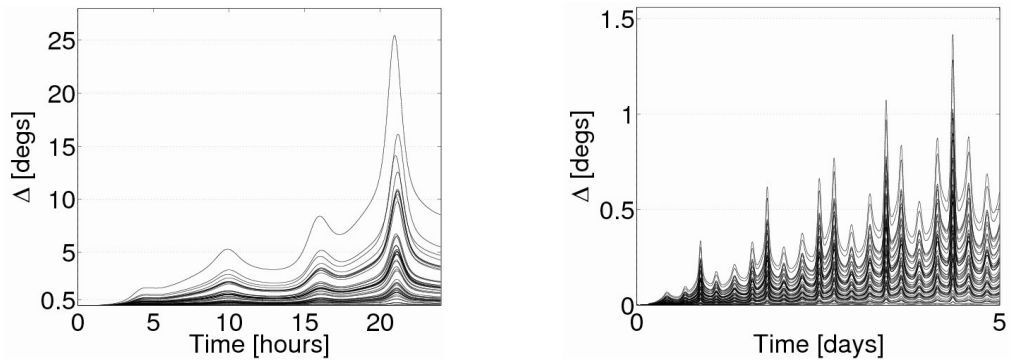

Figure 6: Difference Δ between “true” and elliptical orbit representing the discovery and the first follow-up tracklet (left) and the second follow-up tracklet (right). The curves represent the result of 50 simulations of one object with observation errors statistically distributed within $\sigma = 0.5$”.

For one and the same object the peaks are more or less pronounced depending on the individual Monte Carlo run. We therefore suspect that the large peaks in Figure 3 and Figure 5 are not due to same particular orbits but rather due to statistical observation errors. The peaks have a period of six hours, which corresponds to a half revolution of the object. The time of the peaks might be related to the apogee and perigee passing times of the object.

Third follow-up observation sequence

The results from the previous sections show that the differences get too large for a safe recovery after a few days. A third follow-up tracklet was therefore simulated 24 hours after the discovery for the ESASDT and the ZimSMART. Elliptical orbits were determined using all four observations tracklets. The differences between “true” and the determined orbits are shown in Figure 7 and Figure 8 and the mean formal errors are given in Table 5 (ZimSMART) and Table 6 (ESASDT).

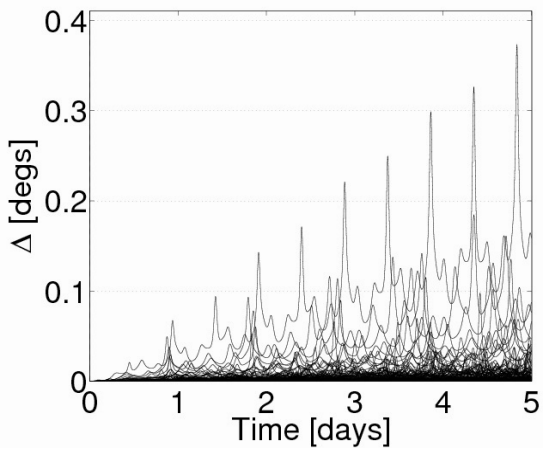

Figure 7: Difference Δ between "true" and elliptical orbit representing the discovery and three follow-up observations for ZimSMART and spanning one day of time. Each curve represents the result for one of the 100 simulated MEO objects.

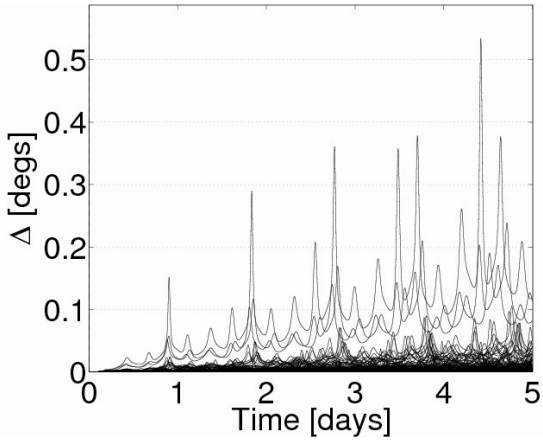

Figure 8: Difference Δ between "true" and elliptical orbit representing the discovery and three follow-up observations for ESASDT and spanning one day of time. Each curve represents the result for one of the 100 simulated MEO objects.

For both telescopes these observation series with three follow-up tracklets and a total arc length of one day allow a successful recovery of all objects after several days. Figure 9 shows the differences for 20 objects observed with ZimSMART extrapolated over 60 days.

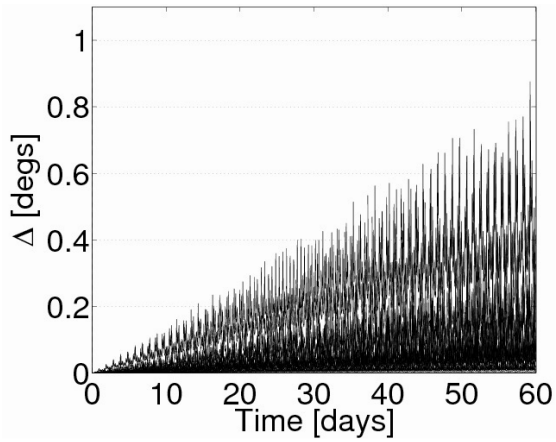

Figure 9: Difference Δ between “true” and elliptical orbit representing the discovery and three follow-up observations spanning one day of time. Each curve represents the result from one of 20 simulations of MEO orbits

Fourth follow-up observation sequence

The present simulations include only a subset of possible scenarios. In general, based on actual experience with observations of GEO and GTO objects, we know that further follow-up tracklets might be necessary to determine a “secured” orbit. Therefore, a fourth follow-up tracklet for both strategies (ESASDT and ZimSMART) was simulated three days after the discovery. All observations have been used again to determine an elliptical orbit. The differences between the determined elliptical orbit and the “true” orbit as a function of time are shown in Figure 10. The differences are slightly worse for the ESASDT strategy (right), but in both cases all objects could be safely recovered up to 60 days after the last follow-up observation. The mean formal errors are given in Table 5 (ZimSMART) and Table 6 (ESASDT).

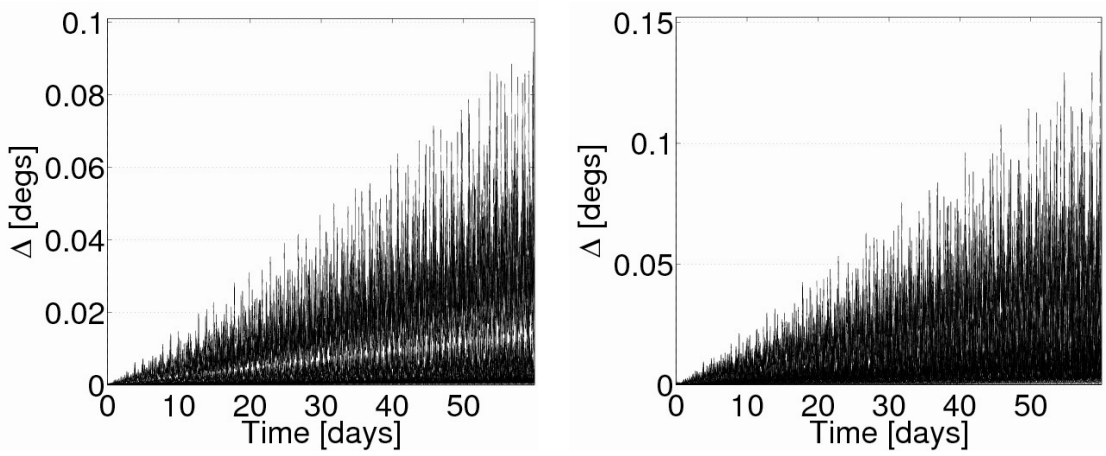

Figure 10: Difference Δ between “true” and elliptical orbit representing the discovery and four follow-up observations spanning three days of time. Each curve represents the result for one of the 100 simulated MEO objetcs. Left (ZimSMART strategy): first follow-up after 1 hour, second after 3 hours, third after 24 hours, fourth after 3 days. Right (ESASDT strategy): first follow-up after 30 minutes, second after 2 hours, third after 24 hours, fourth after 3 days.

Fifth follow-up observation sequence

A fifth follow-up tracklet was simulated 30 days after the discovery observations. A gap of 30 days was chosen according to a reasonable schedule of the observation campaigns. The orbits are shown in Figure 11. There is still a difference between the ESASDT (right) and the ZimSMART (left) strategy.

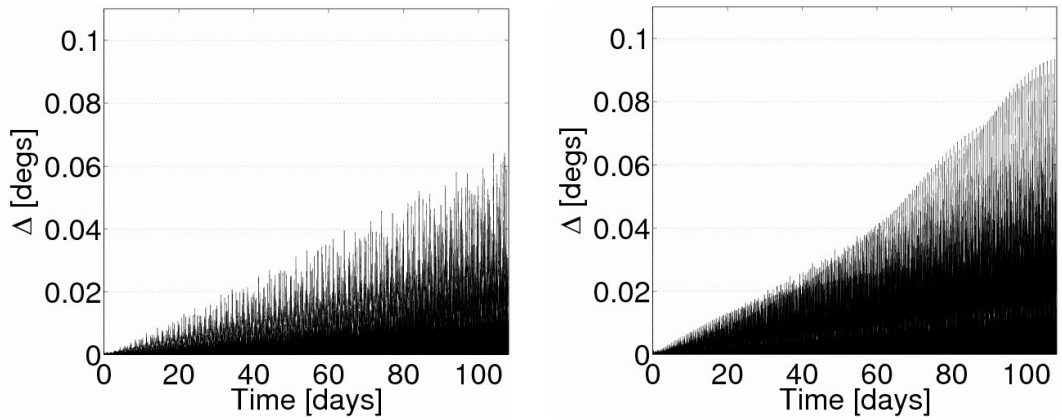

Figure 11: Difference Δ between "true" and elliptical orbit representing the discovery and five follow-up observations spanning 30 days of time**.** Each curve represents the result for one of 50 simulated MEO objects. Left (ZimSMART strategy): first follow-up after 1 hour, second after 3 hours, third after 24 hours, fourth after 3 days, fifth after 30 days. Right (ESASDT strategy): first follow-up after 30 minutes, second after 2 hours, third after 24 hours, fourth after 3 days, fifth after 30 days.

	Arc	*a*	*e*	*i*	Ω	ω	T_0	*m*
3. F-up	24 h	61.5 m	$2.2 \cdot 10^{-6}$	$4.4° \cdot 10^{-5}$	$3.8° \cdot 10^{-5}$	$4.8° \cdot 10^{-2}$	0s	0.3"
4. F-up	3 d	4.7 m	$8.0 \cdot 10^{-7}$	$2.7° \cdot 10^{-5}$	$2.3° \cdot 10^{-5}$	$1.6° \cdot 10^{-2}$	0s	0.29"
5. F-up	30 d	0.9 m	$4.8 \cdot 10^{-7}$	$2.5° \cdot 10^{-5}$	$2.1° \cdot 10^{-5}$	$1.2° \cdot 10^{-1}$	0s	0.29"

Table 5: Mean formal errors of the orbital elements for the elliptical orbit determination representing the third, fourth and fifth follow-up observation with ZimSMART.

	Arc	*a*	*e*	*i*	Ω	ω	T_0	*m*
3. F-up	24 h	70.6 m	$2.9 \cdot 10^{-6}$	$4.8° \cdot 10^{-5}$	$3.9° \cdot 10^{-5}$	$4.3° \cdot 10^{-2}$	0s	0.3"
4. F-up	3 d	7.8 m	$1.7 \cdot 10^{-6}$	$3.1° \cdot 10^{-5}$	$2.3° \cdot 10^{-5}$	$3.5° \cdot 10^{-2}$	0s	0.3"
5. F-up	30 d	1.2 m	$6.6 \cdot 10^{-7}$	$2.6° \cdot 10^{-5}$	$1.9° \cdot 10^{-5}$	$2.2° \cdot 10^{-2}$	0s	0.3"

Table 6: Mean formal errors of the orbital elements for the elliptical orbit determination representing the third, fourth and fifth follow-up observation with ESASDT.

5. Conclusions

Observations of MEO objects for different discovery and follow-up scenarios were simulated. Differences between the "true" orbits and determined orbits based of simulated observations were analysed to assess the performance of the follow-up scenarios. All simulations were done for two specific telescopes, the ESASDT with a FOV of 0.7° and the ZimSMART with a FOV of 4.2°. The results show that after two follow-up observations during the same night the determined orbit has a sufficient accuracy for the successful recovery of a newly detected MEO object in the subsequent night. In many cases the objects can even be recovered after several nights, however, depending on the FOV of the used instrument a third follow-up tracklet might be necessary. In general, the arc covered by the observations should be few hours long for a reliable orbit determination. And "secured" orbits based on observation arcs of a few days can be used to build up a catalogue. The choice of an appropriate follow-up strategy right after the discovery is important for all the subsequent recoveries. The simulations show that the time intervals between the

discovery and the follow-up tracklets may impact the accuracy of the following orbit determinations, even after several months.

The simulations performed in this work cover only a few of many possible scenarios and observation geometries. Depending on time, site, object orbit, and observation constraints, better follow-up strategies might be envisaged. Nevertheless, the results represent a valid starting point for more specific analysis and, give a tint estimate of the time intervals to adopt in the follow-up strategies and the degree of confidence to expect for the object recovery.

6. Acknowledgements

Part of this work was done under ESA contract 21599/08/F/MOS.

7. References

Beutler, G., 'Methods of Celestial Mechanics', Springer, Berlin, 2004.

Musci, R., Schildknecht, T., Ploner, M., 'Orbit improvement for GEO objects using follow-up observations', Advances in Space Research 34, pp. 912-916, 2004.

Musci, R., Schildknecht, T., Ploner, M., Beutler, G., 'Orbit improvement for GTO objects using follow-up observations', Advances in Space Research 35, pp. 1236-1242, 2005.

Musci, R., Schildknecht, T., Beutler, G., Agapov, V., 'Observations of high altitude objects from multiple sites', in: Proceedings of the International Astronautical Congress IAC-06, 2006.

Schildknecht, T., Ploner, M., Hugentobler, U., 'The search for debris in GEO', Advances in Space Research 28, pp. 1291-1299, 2001.

Schildknecht, T., Musci, R., Ploner, M., et al., ,Optical observations of space debris in GEO and in highly-eccentric orbits', Advances in Space Research 34, pp. 901-911, 2004.